

King's Research Portal

DOI:

[10.1016/j.jorganchem.2015.12.023](https://doi.org/10.1016/j.jorganchem.2015.12.023)

Document Version

Peer reviewed version

[Link to publication record in King's Research Portal](#)

Citation for published version (APA):

Chowdhury, M. A. H., Rahman, M. S., Islam, M. R., Rajbangshi, S., Ghosh, S., Hogarth, G., Tocher, D. A., Yang, L., Richmond, M. G., & Kabir, S. E. (2016). Iron carbonyl complexes bearing phenazine and acridine ligands: X-ray structures of $\text{Fe}(\text{CO})_3(\eta^4\text{-C}_3\text{H}_3\text{N}_2)$, $\text{Fe}(\text{CO})_2\{\text{P}(\text{OMe})_2\}(\eta^4\text{-C}_3\text{H}_3\text{N}_2)$, $\text{Fe}(\text{CO})_2(\text{PPh}_2)_2(\eta^4\text{-C}_3\text{H}_3\text{N}_2)$, and $\text{Fe}(\text{CO})_2(\kappa^1\text{-dppm})(\eta^4\text{-C}_3\text{H}_3\text{N}_2)$. *JOURNAL OF ORGANOMETALLIC CHEMISTRY*, 805, 34-41. ^{3 9}
<https://doi.org/10.1016/j.jorganchem.2015.12.023>

Citing this paper

Please note that where the full-text provided on King's Research Portal is the Author Accepted Manuscript or Post-Print version this may differ from the final Published version. If citing, it is advised that you check and use the publisher's definitive version for pagination, volume/issue, and date of publication details. And where the final published version is provided on the Research Portal, if citing you are again advised to check the publisher's website for any subsequent corrections.

General rights

Copyright and moral rights for the publications made accessible in the Research Portal are retained by the authors and/or other copyright owners and it is a condition of accessing publications that users recognize and abide by the legal requirements associated with these rights.

- Users may download and print one copy of any publication from the Research Portal for the purpose of private study or research.
- You may not further distribute the material or use it for any profit-making activity or commercial gain
- You may freely distribute the URL identifying the publication in the Research Portal

Take down policy

If you believe that this document breaches copyright please contact librarypure@kcl.ac.uk providing details, and we will remove access to the work immediately and investigate your claim.

Iron carbonyl complexes bearing phenazine and acridine ligands: X-ray structures of $\text{Fe}(\text{CO})_3(\eta^4\text{-C}_{12}\text{H}_8\text{N}_2)$, $\text{Fe}(\text{CO})_2\{\text{P}(\text{OMe})_3\}(\eta^4\text{-C}_{12}\text{H}_8\text{N}_2)$, $\text{Fe}(\text{CO})_2(\text{PPh}_3)(\eta^4\text{-C}_{13}\text{H}_9\text{N})$, and $\text{Fe}(\text{CO})_2(\kappa^1\text{-dppm})(\eta^4\text{-C}_{12}\text{H}_8\text{N}_2)$

Md. Arshad H. Chowdhury^a, Md. Saifur Rahman^a, Md. Rakibul Islam^a, Subas Rajbangshi^a, Shishir Ghosh^a, Graeme Hogarth^b, Derek A. Tocher^c, Li Yang^d, Michael G. Richmond^d, Shariff E. Kabir^{a,*}

^a*Department of Chemistry, Jahangirnagar University, Savar, Dhaka 1342, Bangladesh*

^b*Department of Chemistry, King's College London, Britannia House, 7 Trinity Street, London SE1 1DB, UK*

^c*Department of Chemistry, University College London, 20 Gordon Street, London WC1H 0AJ, UK*

^d*Department of Chemistry, University of North Texas, Denton, TX 76209, USA*

* Corresponding author.

E-mail address: skabir_ju@yahoo.com (S.E. Kabir).

Tel.: +880 27791099; fax: +880 27791052.

Abstract

Reactions of $\text{Fe}_3(\text{CO})_{12}$ with the heterocycles phenazine and acridine in refluxing benzene afforded the mononuclear complexes $\text{Fe}(\text{CO})_3(\eta^4\text{-C}_{12}\text{H}_8\text{N}_2)$ (**1a**) and $\text{Fe}(\text{CO})_3(\eta^4\text{-C}_{13}\text{H}_9\text{N})$ (**1b**), respectively. Treatment of **1a** with $\text{P}(\text{OMe})_3$ and PPh_3 in the presence of Me_3NO at room temperature yielded the carbonyl substitution products $\text{Fe}(\text{CO})_2\{\text{P}(\text{OMe})_3\}(\eta^4\text{-C}_{12}\text{H}_8\text{N}_2)$ (**2a**) and $\text{Fe}(\text{CO})_2(\text{PPh}_3)(\eta^4\text{-C}_{12}\text{H}_8\text{N}_2)$ (**3a**), respectively. Similar reactions of **1b** yielded $\text{Fe}(\text{CO})_2\{\text{P}(\text{OMe})_3\}(\eta^4\text{-C}_{13}\text{H}_9\text{N})$ (**2b**) and $\text{Fe}(\text{CO})_2(\text{PPh}_3)(\eta^4\text{-C}_{13}\text{H}_9\text{N})$ (**3b**). Treatment of **1a** with the diphosphines *dppm* and *dppf* under similar conditions afforded the mononuclear compounds $\text{Fe}(\text{CO})_2(\kappa^1\text{-dppm})(\eta^4\text{-C}_{12}\text{H}_8\text{N}_2)$ (**4a**) and $\text{Fe}(\text{CO})_2(\kappa^1\text{-dppf})(\eta^4\text{-C}_{12}\text{H}_8\text{N}_2)$ (**4b**). Compounds **1a**, **2a**, **3b**, and **4a** have been structurally characterized by X-ray crystallography. The ancillary phenazine and acridine ligands in these products adopt an η^4 -coordination mode by using only the peripheral carbon atoms in one of the carbocyclic rings. Given the rarity of this coordination mode in metal carbonyl complexes, we have performed electronic structure calculations on **1a** and these data are discussed relative to the solid-state structure.

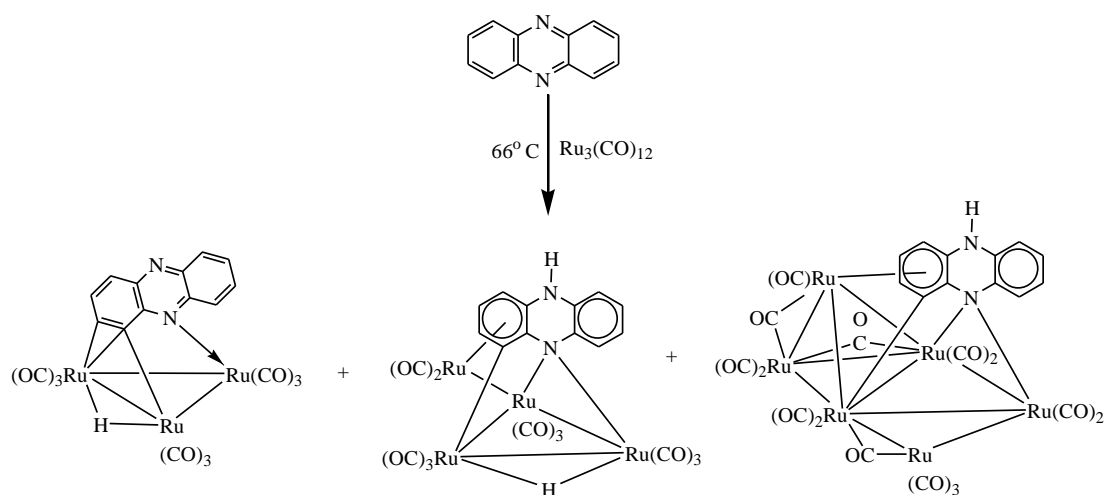
Keywords: Iron carbonyl; Phenazine; Acridine; Phosphines; X-ray structure; DFT calculations

1. Introduction

Phenazine, a bisannulated derivative of pyrazine, is a planar *N*-heterocyclic ligand whose biological and spectral properties have been extensively studied in the fields of chemistry and biology.^{1,2,3,4,5,6,7,8} Although similar to the parent heterocycle, pyrazine, with respect to its N-based coordination chemistry, it has different electronic and steric properties, which in turn give rise to ligand coordination modes and unique structural motifs for those compounds that possess an ancillary phenazine. Phenazine possesses idealized C_{2h} symmetry similar to pyrazine, but the presence of the fused benzene rings at the [2,3-b] and [5,6-e] pyrazine junctions imparts additional steric bulk to phenazine related to the parent heterocycle and the monoannulated derivative quinoxaline. As an ancillary ligand, phenazine is known to exhibit terminal⁹ and bridging¹⁰ coordination modes, as well as functioning as an electron donor in intermolecular arrays by directing the formation of columnar stacks through π - π interactions.¹¹ Acridine contains only one nitrogen atom and its structural properties and reactivity often mimic that of phenazine.

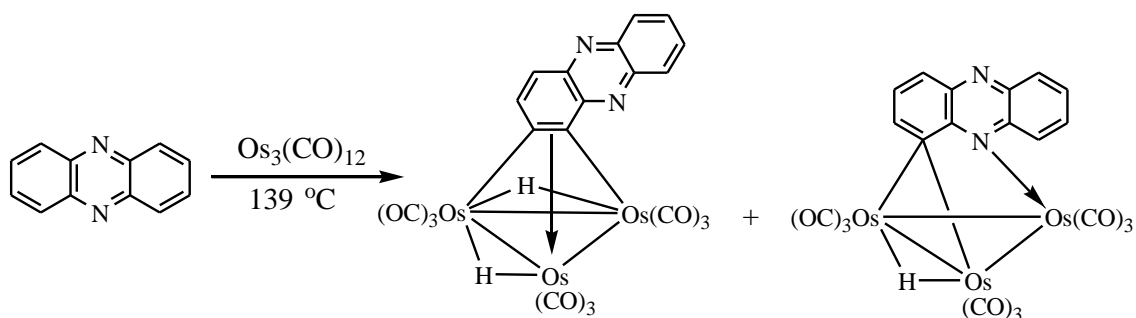
The ligand substitution chemistry displayed by the trimetal clusters $M_3(CO)_{12-n}(MeCN)_n$ (where $M = Fe, Ru, Os$; $n = 0, 1, 2$) typically reveals great diversity in reactivity and structural outcome between the Fe_3 versus the Ru_3 and Os_3 analogs.¹² Of the numerous substrates investigated in such substitution reactions, nitrogen-containing heterocycles have received considerable attention. The driving force behind these studies is attributed to industrial demands for selective and catalytic transformations of commonplace heterocyclic substrates to high-value commodity chemicals. This interest is further supplemented by the increased importance for industrial hydrodenitration of crude oil feedstocks that are employed in the production of higher value petroleum distillates.¹³

While the reactivity of the triruthenium and triosmium clusters $M_3(CO)_{12-n}(MeCN)_n$ with the nitrogen heterocycles pyridine,^{14,15,16,17} pyrazole,¹⁴ pyrimidine,^{18,19} pyrazine,^{18,20} quinoxaline,²⁰ and quinoline^{18,21,22,23} has been extensively investigated, few studies have hitherto been published involving the heterocycle phenazine. Cabeza et al.²⁴ recently reported that the reaction of $Ru_3(CO)_{12}$ with phenazine in refluxing THF led to the formation of tri-, tetra- and hexanuclear clusters $Ru_3(CO)_9(\mu_3\text{-}\{(C_6H_4)(C_6H_3)N_2\})(\mu\text{-H})$, $Ru_4(CO)_{10}(\mu\text{-CO})(\mu_4\text{-}\{(C_6H_4)(C_6H_3)N_2H\})$ and $Ru_6(CO)_{12}(\mu\text{-CO})(\mu_5\text{-}\{(C_6H_4)(C_6H_3)N_2H\})$ (Scheme 1).



Scheme 1.

More recently, we reported the isolation and structural characterization of the face-capped monohydride $Os_3(CO)_9(\mu_3\text{-}\eta^2\text{-}C_{12}H_7N_2)(\mu\text{-H})$ and electron-precise dihydride $Os_3(CO)_9(\mu_3\text{-}\eta^2\text{-}C_{12}H_6N_2)(\mu\text{-H})_2$ clusters from the reaction of $Os_3(CO)_{12}$ with phenazine in refluxing xylene (Scheme 2).²⁵



Scheme 2.

In order to complete the study of phenazine reactivity with the Group 8 trimetallic clusters, we have investigated the reaction of $\text{Fe}_3(\text{CO})_{12}$ with phenazine. Herein, we report our results on the mononuclear iron compound $\text{Fe}(\text{CO})_3(\eta^4\text{-C}_{12}\text{H}_8\text{N}_2)$ (**1a**), which was isolated from the thermolysis of $\text{Fe}_3(\text{CO})_{12}$ in the presence of phenazine. Also reported is the reactivity of acridine with $\text{Fe}_3(\text{CO})_{12}$ under analogous conditions, which furnishes $\text{Fe}(\text{CO})_3(\eta^4\text{-C}_{13}\text{H}_9\text{N})$ (**1b**). Our data reveal that the two heterocyclic ligands adopt a different coordination mode in the case of iron compared to the products found in the related reactions using ruthenium and osmium carbonyl cluster complexes.

2. Experimental

2.1. General procedures

Unless otherwise noted, all reactions were carried out under a nitrogen atmosphere using standard Schlenk techniques. Reagent-grade solvents were dried using appropriate drying agents and distilled prior to use by standard methods. $\text{Fe}_3(\text{CO})_{12}$ was prepared according to the published procedure.²⁶ Phenazine and acridine were purchased from Sigma-Aldrich and used without further purification. $\text{Me}_3\text{NO}\cdot 2\text{H}_2\text{O}$ was dried by azeotropic distillation using benzene with Dean–Stark distillation equipment. Infrared spectra were recorded on a Shimadzu IR Prestige-21 spectrophotometer, and the ^1H and ^{13}C NMR spectra were recorded on a Varian Unity 500 NMR spectrometer. The spectral assignments for **1a** were ascertained through a combination of 2D NMR experiments, including ^1H COSY, HMQC, and HMBC techniques. All chemical shifts are reported in δ units and are referenced to the residual protons of the deuterated solvents (^1H and ^{13}C) and external 85% H_3PO_4 (^{31}P) as appropriate. Elemental analyses were performed by the Microanalytical Laboratories of the Wazed Miah Science Research Centre at Jahangirnagar University. Product separations were performed by TLC in air on 0.5 mm silica gel (GF₂₅₄-type 60, E. Merck, Germany) glass plates.

2.2. Reaction of $Fe_3(CO)_{12}$ with phenazine

A benzene solution (25 mL) containing $Fe_3(CO)_{12}$ (0.20 g, 0.40 mmol) and phenazine (71 mg, 0.39 mmol) was heated to reflux for 3 h. The solvent was removed under reduced pressure and the residue chromatographed by TLC on silica gel. Elution with cyclohexane/ CH_2Cl_2 (2:3, v/v) developed four bands. The slowest moving band afforded $Fe(CO)_3(\eta^4-C_{12}N_2H_8)$ (**1a**) (0.18 g, 47%) as orange crystals after recrystallization from dichloromethane/hexane at 4 °C. The first and second bands were too small for complete characterization, while the third band afforded unreacted phenazine. Spectral data for **1a**: IR (ν_{CO} , CH_2Cl_2): 2064 vs, 2005 vs, 1997 sh cm^{-1} . 1H NMR (CD_2Cl_2): δ 3.87 (AA', diene, J = 5.4, 3.5 Hz, 2H), 6.53 (XX', diene, J = 5.4, 3.5 Hz, 2H), 7.38 (AA', aryl, J = 6.5, 3.0 Hz, 2H), 7.51 (BB', J = 6.5, 3.0 Hz, 2H). ^{13}C NMR (CD_2Cl_2): δ 62.14 (CH), 88.03 (CH), 127.55 (CH), 128.18 (CH), 139.46 (C), 156.98 (C), 207.25 (Fe-CO). Anal. Calcd. for $C_{15}H_8FeN_2O_3$: C, 56.29; H, 2.52; N, 8.75. Found: C, 56.55; H, 2.72; N, 8.83%. A similar reaction between $Fe_2(CO)_9$ (50 mg, 0.14 mmol) and phenazine (25 mg, 0.14 mmol), followed by similar chromatographic separation, afforded **1a** (18 mg, 20%), while use of $Fe(CO)_5$ (50 mg, 0.26 mmol) as the iron precursor (46 mg, 0.26 mmol) also furnished **1a** (15 mg, 18%).

2.3 Reaction of $Fe_3(CO)_{12}$ with acridine

A benzene solution (25 mL) of $Fe_3(CO)_{12}$ (0.10 g, 0.20 mmol) and acridine (0.11 g, 0.59 mmol) was heated to reflux for 1.5 h and then allowed to cool to room temperature. The solvent was removed under reduced pressure and the residue chromatographed by TLC on silica gel. Elution with cyclohexane/acetone (4:1, v/v) developed four bands. The third band gave $Fe(CO)_3(\eta^4-C_{13}H_9N)$ (**1b**) (66 mg, 35%) as orange crystals after recrystallization from hexane/ CH_2Cl_2 at 4 °C. The first and the fourth bands corresponded to unreacted $Fe_3(CO)_{12}$ and acridine, respectively. The second band was too small for complete characterization. Spectral data for **1b**: IR (ν_{CO} , CH_2Cl_2): 2057 vs, 1995 s, 1983 sh cm^{-1} . 1H NMR ($CDCl_3$): δ 7.65 (d, 1H, J = 5.5 Hz), 7.41 (d, 2H, J = 7.2 Hz), 7.28 (s, 1H), 7.14 (s, 1H), 6.56 (s, 1H), 6.40 (s, 1H), 3.88 (s, 1H), 3.77 (s, 1H). Anal. Calcd. for $C_{16}H_9FeNO_3$: C, 60.22; H, 2.84; N, 4.39. Found: C, 60.42; H, 3.05; N, 4.58%.

2.4. Reaction of **1a** with $P(OMe)_3$

To a dichloromethane solution (20 mL) of **1** (20 mg, 0.06 mmol) and P(OMe)₃ (15 μL, 0.12 mmol) was added dropwise a solution of Me₃NO (5 mg, 0.01 mmol) in the same solvent (10 mL) and the solution was stirred at room temperature for 2h. The solution was then filtered through a short silica column (4 cm), followed by solvent removal under reduced pressure. The resulting residue was purified by chromatography over silica gel using cyclohexane/CH₂Cl₂ (1:9, v/v) as the eluent. Of the two developed two bands, the faster moving band corresponded to unconsumed **1a** (trace), while the slower moving band yielded Fe(CO)₂{P(OMe)₃}(η^4 -C₁₂H₈N₂) (**2a**) (23 mg, 88%). The analytical sample of **2a** was isolated as red crystals after recrystallization from hexane/CH₂Cl₂ at 4 °C. Spectral data for **2a**: IR (νCO, CH₂Cl₂): 2008 vs, 1954 vs cm⁻¹. ¹H NMR (CDCl₃): δ 7.47 (m, 2H), 7.31 (m, 2H), 6.23 (m, 2H), 3.62 (m, 2H), 3.58 (d, *J* = 15.0 Hz, 9H). ³¹P{¹H}NMR (CDCl₃): δ 174.6 (s). Anal. Calcd. for C₁₇H₁₇FeN₂O₅P: C, 49.07; H, 4.12; N, 6.73. Found: C, 49.22; H, 4.28; N, 6.88%.

2.5. Reaction of **1b** with P(OMe)₃

A similar reaction between **1b** (20 mg, 0.06 mmol) and P(OMe)₃ (15 μL, 0.12 mmol) in the presence of Me₃NO (10 mg, 0.01 mmol) yielded Fe(CO)₂{P(OMe)₃}(η^4 -C₁₃H₉N) (**2b**) (21 mg, 80%) as red crystals after recrystallization from hexane/CH₂Cl₂ at 4 °C. Spectral data for **2b**: IR (νCO, CH₂Cl₂): 1999 (vs), 1943 (vs) cm⁻¹. ¹H NMR (CDCl₃): δ 7.58 (d, *J* = 8.4 Hz, 1H), 7.32 (t, *J* = 8.0 Hz, 2H), 7.19 (t, *J* = 8.0 Hz, 1H), 6.97 (s, 1H), 6.23 (s, 1H), 6.08 (s, 1H), 3.61 (m, 1H), 3.58 (d, *J* = 11.6 Hz, 9H), 3.45 (d, *J* = 6.0 Hz, 1H). ³¹P{¹H}NMR (CDCl₃): δ 177.1 (s). Anal. Calcd. for C₁₈H₁₈FeNO₅P: C, 52.08; H, 4.37; N, 3.37. Found: C, 52.28; H, 4.55; N, 3.48%.

2.6. Reaction of **1a** with PPh₃

To a dichloromethane solution (20 ml) of **1a** (40 mg, 0.13 mmol) and triphenylphosphine (33 mg, 0.126 mmol) was added dropwise a CH₂Cl₂ solution containing Me₃NO (10 mg, 0.013 mmol), followed by stirring at room temperature for 2h. Filtration of the crude reaction mixture through a short silica column (4 cm), followed by solvent removal, afforded the crude product. Chromatographic purification using cyclohexane/dichloromethane (2:3, v/v) developed four bands, of which the first band was confirmed as unreacted triphenylphosphine. The second band was too small for complete characterization and the third band was phenazine (trace). The fourth band gave the desired product [Fe(CO)₂(PPh₃)(η^4 -C₁₂H₈N₂)] (**3a**) (66 mg, 95%) as red crystals after recrystallization from

dichloromethane/hexane at 4 °C. Spectral data for **3a**: IR (ν_{CO} , CH_2Cl_2): 1997 (vs), 1943 (vs) cm^{-1} . ^1H NMR (CDCl_3): δ 7.44 (m, 17H), 7.39 (m, 2H), 5.98 (m, 2H), 3.30 (m, 2H). $^{31}\text{P}\{^1\text{H}\}$ NMR (CDCl_3): δ 67.0 (s). Anal. Calcd. for $\text{C}_{32}\text{FeH}_{23}\text{N}_2\text{O}_2\text{P}$: C, 69.30; H, 4.18; N, 5.05. Found: C, 69.60; H, 4.40; N, 5.15%.

2.7. Reaction of **1b** with PPh_3

A similar reaction between **1b** (26 mg, 0.08 mmol) and triphenylphosphine (21 mg, 0.08 mmol) in the presence of Me_3NO (6 mg, 0.08 mmol) was conducted and $\text{Fe}(\text{CO})_2(\text{PPh}_3)(\eta^4\text{-C}_{13}\text{H}_9\text{N})$ (**3b**) (40 mg, 88%) was isolated as red crystals after recrystallization from dichloromethane/hexane at 4 °C. Spectral data for **3b**: IR (ν_{CO} , CH_2Cl_2): 1988 (vs), 1933 (vs) cm^{-1} . ^1H NMR (CDCl_3): δ 7.60 (d, $J = 8.0$ Hz, 1H), 7.43 (m, 15H), 7.33 (t, $J = 8.0$ Hz, 2H), 7.19 (t, $J = 8.0$ Hz, 1H), 6.84 (s, 1H), 6.06 (s, 1H), 5.90 (s, 1H), 3.38 (s, 1H), 2.98 (s, 1H). $^{31}\text{P}\{^1\text{H}\}$ NMR (CDCl_3): δ 66.6 (s). Anal. Calcd. for $\text{C}_{33}\text{H}_{24}\text{FeNO}_2\text{P}$: C, 71.62; H, 4.37; N, 2.53. Found: C, 71.79; H, 4.46; N, 5.56%.

2.9. Reaction of **1a** with *dppm*

To a dichloromethane solution of **1a** (20 mg, 0.06 mmol) and *dppm* (24 mg, 0.06 mmol) was added dropwise a solution of Me_3NO (5 mg, 0.006 mmol) in the same solvent (10 mL) and stirring continued for 2 h at room temperature. The solution was filtered through a short silica column (4 cm), after which time the solvent was removed under reduced pressure and the residue chromatographed by TLC on silica gel. Elution with cyclohexane/ CH_2Cl_2 (1:9, v/v) developed two bands. The faster moving band afforded $\text{Fe}(\text{CO})_2(\kappa^1\text{-dppm})(\eta^4\text{-C}_{12}\text{H}_8\text{N}_2)$ (**4a**) (18 mg, 40%) and slower moving band was isolated in an insufficient amount for spectroscopic characterization. Spectral data for **4a**: IR (ν_{CO} , CH_2Cl_2): 1996 (vs), 1942 (vs) cm^{-1} . ^1H NMR(CDCl_3): δ 7.36 (m, 6H), 7.28 (m, 18H), 6.04 (m, 4H), 3.23 (m, 1H), 3.04 (m, 1H). $^{31}\text{P}\{^1\text{H}\}$ NMR (CDCl_3): δ 57.5 (d, $J = 76.0$ Hz, 1P), -24.2 (d, $J = 76.0$ Hz, 1P). Anal. Calcd. for $\text{C}_{39}\text{H}_{30}\text{FeN}_2\text{O}_2\text{P}_2$: C, 69.25; H, 4.47; N, 4.14. Found: C, 69.42; H, 4.62; N, 4.32%.

2.8. Reaction of **1a** with *dppf*

To a dichloromethane solution (20 mL) of **1a** (20 mg, 0.06 mmol) and *dppf* (35 mg, 0.06 mmol) was added dropwise a CH_2Cl_2 solution (10 mL) of Me_3NO (5 mg, 0.06 mmol) over a period of 30 min and stirred for an additional 5 h at room temperature. The reaction mixture was then filtered through a short silica column (4 cm). The solvent was removed under reduced pressure and the residue chromatographed by TLC on silica gel. Elution with

cyclohexane/dichloromethane (3:7, v/v) developed four bands. The first and second bands were unreacted dppf and phenazine, respectively. The third gave $\text{Fe}(\text{CO})_2(\kappa^1\text{-dppf})(\eta^4\text{-C}_{12}\text{H}_8\text{N}_2)$ (**5a**) (21 mg, 40%) while the fourth band afforded a trace amount of material insufficient for characterization. Spectral data for **5a**: IR (νCO , CH_2Cl_2): 1994(vs), 1941(vs) cm^{-1} . ^1H NMR (CDCl_3): δ 7.43 (m, 20H), 7.23 (m, 4H), 5.91 (m, 2H), 4.45 (m, 2H), 4.22 (m, 2H), 3.86 (m, 2H), 3.70 (m, 2H), 3.06 (m, 2H). $^{31}\text{P}\{^1\text{H}\}$ NMR (CDCl_3): δ 61.0 (s, 1P) -18.1 (s, 1P). Anal. Calcd. for $\text{C}_{48}\text{H}_{36}\text{Fe}_2\text{N}_2\text{O}_2\text{P}_2$: C, 68.11; H, 4.29; N, 3.31. Found: C, 68.31; H, 4.42; N, 3.46%.

2.9. X-ray crystallography

2.10. Computational details and modeling

The DFT calculations on $\text{Fe}(\text{CO})_3(\eta^4\text{-C}_{12}\text{H}_8\text{N}_2)$ (species **A**) were carried out with the Gaussian 09 package of programs,²⁷ using the B3LYP hybrid functional. This functional is comprised of Becke's three-parameter hybrid exchange functional (B3)²⁸ and the correlation functional of Lee, Yang, and Parr (LYP).²⁹ The iron atom was described with the Stuttgart-Dresden effective core potential and SDD basis set,³⁰ and the 6-31G(d') basis set³¹ was employed for all remaining atoms.

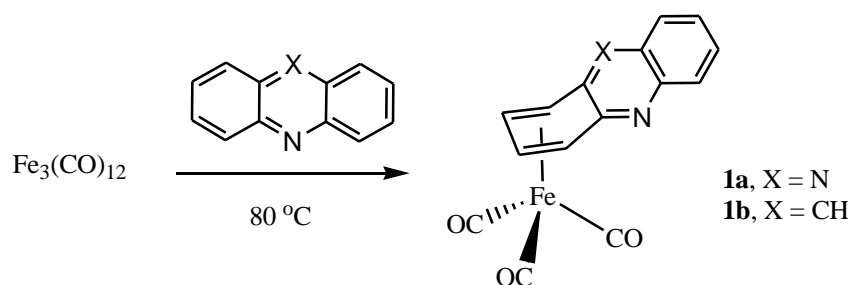
The reported geometry for **A** was fully optimized and the analytical second derivatives were evaluated, confirming that the geometry was an energy minimum (no negative eigenvalues). Unscaled vibrational frequencies were used to make zero-point and thermal corrections to the electronic energies. The computed harmonic frequencies for the carbonyl stretching bands have been scaled using a scaling factor of 0.965. The natural charges and Wiberg indices were computed using Weinhold's natural bond orbital (NBO) program.^{32,33} The geometry-optimized structures have been drawn with the *JIMP2* molecular visualization and manipulation program.³⁴

3. Results and discussion

3.1. Reactions of $\text{Fe}_3(\text{CO})_{12}$ with phenazine and acridine

Treatment of $\text{Fe}_3(\text{CO})_{12}$ with phenazine and acridine in refluxing benzene afforded the mononuclear complexes $\text{Fe}(\text{CO})_3(\eta^4\text{-C}_{12}\text{N}_2\text{H}_8)$ (**1a**) (47% yield) and $\text{Fe}(\text{CO})_3(\eta^4\text{-C}_{13}\text{H}_9\text{N})$ (**1b**) (35% yield), respectively, which were isolated as yellow crystals after chromatographic workup. Both new compounds **1a** and **1b** have been characterized by a combination of

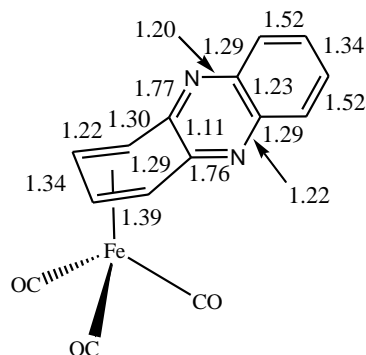
elemental analysis, IR, and ^1H NMR spectroscopy; the solid-structure of **1a** was also determined by single crystal X-ray diffraction analysis.



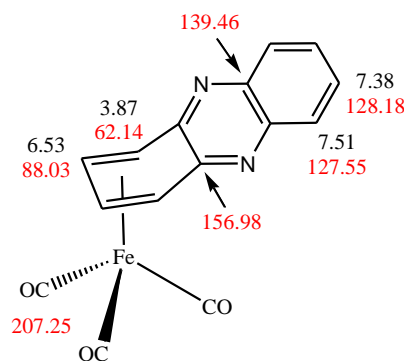
Scheme 3

The ORTEP drawing of the molecular structure of **1a** is depicted in Fig. 1 (top) and selected bond distances and angles are reported in the figure caption. The molecule contains one iron atom whose coordination sphere consists of three carbonyl ligands and an η^4 - $\text{C}_{12}\text{H}_8\text{N}_2$ ligand. The η^4 coordination of the phenazine in **1a** represents a rare bonding mode for this ligand. While η^4 -phenazine ligands have been structurally demonstrated by Parkin et al.³⁵ in a series of molybdenum compounds and by Yang et al.³⁶ for one nickel diamine complex, no entries of mononuclear iron compounds exist in the Cambridge Structural Database (CSD version 5.36, November 2014). To our knowledge, the iron compounds reported here represent the first such examples that reveal the η^4 coordination of phenazine and acridine ligands. **1a** contains 18e and is electronically saturated, with the CO groups and diene moiety contributing a total of 6e and 4e, respectively to the total electron count. The orientation of the ancillary CO groups relative to the coordinated phenazine is not unlike that found in structurally characterized iron and ruthenium $\text{M}(\text{CO})_3(\eta^4\text{-diene})$ compounds.³⁷ The theoretical basis for the preferred disposition of the $\text{Fe,Ru}(\text{CO})_3$ rotor relative to the polyene framework has been previously addressed.³⁸ The mean Fe-C bond distance of 2.056 Å for the outer carbon atoms associated with the diene moiety [Fe(1)-C(5) and Fe(1)-C(6)] is 0.101 Å shorter than the mean Fe-C distance for the inner Fe-C(diene) vectors [Fe(1)-C(4) and Fe(1)-C(7)]. Another important aspect of the structure is, as expected, the carbon-carbon bond distances of the coordinated benzo ring [C(4)-C(5) 1.430(3), C(6)-C(7) 1.425(3), Å] are longer than those of the uncoordinated benzo ring [C(10)-C(11) 1.403(3), C(11)-C(12) 1.414(3), C(12)-C(13) 1.377(3), C(13)-C(14) 1.393(3), C(14)-C(15) 1.376(3), C(15)-C(10) 1.412(3) Å]. The C-N bond distances involving coordinated benzo group [N(1)-C(8) 1.308(2), N(2)-C(9) 1.312(2) Å] are shorter than those of the uncoordinated benzo ring [N(1)-C(11) 1.386(2), N(2)-C(10) 1.394(2) Å]. The DFT

optimized structure of **A** is depicted below that of **1a** in Figure 1, and an excellent correspondence exists between the two structures. The Wiberg bond indices (WBI) computed for the heterocyclic scaffold (shown below) parallel the experimentally determined bond lengths and underscore the bond length alterations depicted by the resonance contributor of **1a** in Scheme 3.



The solution spectroscopic data of **1a** are in complete agreement with the solid-state structure. The infrared spectrum of **1a** recorded in CH_2Cl_2 reveals three terminal $\nu(\text{CO})$ bands at 2065, 2005, and 1997 cm^{-1} , of which the highest energy band corresponds to the symmetric stretching mode for the three vibrationally coupled carbonyl groups. The remaining two $\nu(\text{CO})$ bands represent different combinations of antisymmetric stretches involving the carbonyl groups. The nature of these assignments was ascertained by normal mode analysis of the frequency data from the DFT-optimized structure. The ^1H NMR spectrum of **1a** (recorded in CD_2Cl_2) shows two different sets of symmetrical spin systems for the eight hydrogens. The diene moiety appears as an AA'XX' system with multiplets centered at δ 3.87 and 6.53, while the remaining four hydrogens on the iron-free aryl ring appear as an AA'BB' spin system. The specific assignments in these spin systems were verified by ^1H COSY measurements and the coupling constants were established by spectral simulation using the available program gNMR. The ^{13}C NMR spectrum reveals eight ^{13}C resonances, of which the seven that appear from δ 62.14 to 156.98 belong to the phenazine ligand that possesses idealized C_s symmetry. Rapid tripodal rotation of three CO groups leads to a time-averaged resonance at δ 207.25.³⁹ The ^{13}C spectral assignments were determined by a combination of HMQC and HMBC experiments, and the below picture shows the specific ^1H (black) and ^{13}C (red) NMR assignments for **1a**. The IR and ^1H spectral data recorded for **1b** were similar in nature and are summarized in the experimental section.

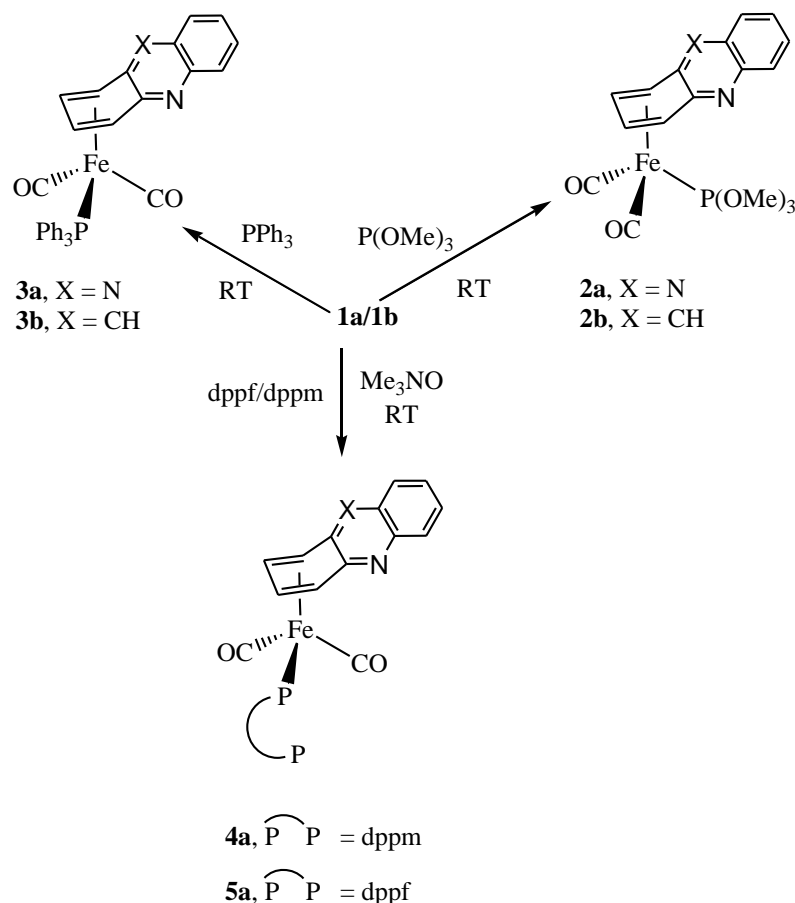


3.2. Reactions of **1a** and **1b** with monodentate phosphines

The ligand substitution reactivity of **1a** and **1b** was next explored as a check of the lability of the coordinated heterocycle in the presence of P-donors. Trimethylamine N-oxide initiated reactions of **1a** with trimethylphosphite and triphenylphosphine at room temperature afforded the mono-substituted products $\text{Fe}(\text{CO})_2\{\text{P}(\text{OMe})_3\}(\eta^4\text{-C}_{12}\text{H}_8\text{N}_2)$ (**2a**) and $\text{Fe}(\text{CO})_3(\text{PPh}_3)(\eta^4\text{-C}_{12}\text{H}_8\text{N}_2)$ (**3a**) as red crystals in 88 and 95% yields, respectively. The reaction of **1b** with $\text{P}(\text{OMe})_3$ and PPh_3 proceeded similarly and furnished $\text{Fe}(\text{CO})_2\{\text{P}(\text{OMe})_3\}(\eta^4\text{-C}_{13}\text{H}_9\text{N})$ (**2b**) (80% yield) and $\text{Fe}(\text{CO})_3(\text{PPh}_3)(\eta^4\text{-C}_{13}\text{H}_9\text{N})$ (**3b**) (88% yield), respectively. Attempts to substitute a second carbonyl in the initial substitution products **2a,b** and **3a,b** by either PPh_3 or $\text{P}(\text{OMe})_3$ in the presence of Me_3NO were unsuccessful. In no case was any evidence for the release of the heterocyclic ligand observed.

The data obtained from elemental analyses and IR and NMR spectroscopies corroborate the nature of the products **2a,b** and **3b**, whose structures are depicted in Scheme 4. Moreover, the solid-state structures of **2a** and **3b** were also established by X-ray crystallography. The ORTEP drawing of molecular structure of **2a** is depicted in Fig. 2, confirming the substitution of a single CO ligand by $\text{P}(\text{OMe})_3$ and whose presence is shown to lie underneath the coordinated phenazine ligand. The figure caption lists selected bond distances and angles for **2a**. The Fe-C(phenazine) bond distances [Fe(1)-C(7) 2.048(4), Fe(1)-C(8) 2.050(4), Fe(1)-C(6) 2.153(4), Fe(1)-C(9) 2.153(4) Å] are comparable in length to those Fe-C bonds in **1a**. The C-C bond lengths in the diene portion of the ligand [C(6)-C(7) 1.428(5), C(7)-C(8) 1.408(5), C(8)-C(9) 1.423(5) Å] are shorter than those carbon-carbon bond lengths associated with the non-coordinated aryl ring [C(6)-C(17) 1.472(5), C(9)-C(10) 1.453(5) Å]. The Fe-P vector exhibits a distance is 2.1647(6) Å, which in turn is intermediate in length compared to the Fe-P bond distance in $[\text{Fe}(\text{CO})(\text{COMe})(\eta^5\text{-MeC}_5\text{H}_4)(\text{PPh}_2\text{Et})]$ {2.200(2) Å}⁴⁰ and $[\text{Fe}(\text{CO})\{\eta^1\text{-C}(\text{O})\text{C}(\text{Me})=\text{C}(\text{Ph})\text{Me}\}(\eta^5\text{-C}_5\text{H}_5)(\text{P}(\text{OPh})_3)]$ {2.110(1) Å}.⁴¹

The ORTEP drawing of the molecular structure of **3b** is shown in Fig. 3. The molecule is structurally similar to **2a** apart from the terminal PPh₃ ligand and the η⁴-acridine ligand. The coordinated PPh₃ adopts one of the two coordination sites at iron that are distal to the heterocycle. The acridine ligand is coordinated to the iron atom in a manner analogous to that of the phenazine ligand in **1a** and **2a**. The Fe-P bond distance is 2.2277(6) Å and is significantly longer than the Fe-P bond distance in **2a**.



Scheme 4

The IR spectra of compounds **2a,b** and **3a,b** display, as expected, two strong carbonyl stretching frequencies (**2a**: 2008, 1954 cm⁻¹; **2b**: 1999, 1943 cm⁻¹; **3a**: 1997, 1943 cm⁻¹; **3b**: 1988, 1933 cm⁻¹), indicating that the number and arrangement of CO ligands are similar in the four Fe(CO)₂P(η⁴-polyene) species. The shifts of the stretching frequencies to lower wavenumbers going from **1a** and **1b** to **2a,b** and **3a,b** are consistent with increased electron density at the iron center from the replacement of a carbonyl ligand with a P-donor ligand. The ³¹P NMR spectrum of each compound displays a single resonance at δ 174.6 (**2a**), 177.1 (**2b**), 67.0 (**3a**), and 66.6 (**3b**) for the coordinated phosphite/phosphine ligand. The presence

of AA'XX' and AA'BB' multiplets in the ^1H NMR spectrum of **2a** are confirmed for the diene and non-coordinated aryl ring protons, and the doublet at δ 3.58 (9H) is readily ascribed to the methyl protons of the $\text{P}(\text{OMe})_3$ ligand. The recorded ^1H NMR data for **2b** are consistent with the proposed structure. Use of PPh_3 as a ligand in the substitution reactions with **1a,b** afforded products similar to those of **2a,b**, and these data are summarized in the experimental section.

3.3. Reactions of **1a** with diphosphines

The reactivity of **1a** with the diphosphines dppm and dppf were next examined in order to probe the ligand chelation of these diphosphines at the iron center. Heating **1a** with dppm at 40 °C in the presence of Me_3NO afforded the mononuclear complex $\text{Fe}(\text{CO})_2(\kappa^1\text{-dppm})(\eta^4\text{-C}_{12}\text{H}_8\text{N}_2)$ (**4a**) in 40% yield. A comparable product yield was also obtained when the more flexible dppf was employed, furnishing $\text{Fe}(\text{CO})_2(\kappa^1\text{-dppf})(\eta^4\text{-C}_{12}\text{H}_8\text{N}_2)$ (**5a**) in 50% yield. Compounds **4a** and **5a** have been characterized by a combination of elemental analysis, IR, ^1H and $^{31}\text{P}\{^1\text{H}\}$ NMR spectroscopies, and by single crystal X-ray diffraction analysis in the case of **4a**. An ORTEP drawing of the molecular structure of **4a** is depicted in Fig. 4 and selected bond distances and angles are reported in the figure caption. The structure of **4a** confirms the replacement of a single CO in **1a** and the presence of a κ^1 -coordinated dppm ligand. The Fe-C bond distances to the phenazine ligand [$\text{Fe}(1)\text{-C}(3) = 2.122(4)$, $\text{Fe}(1)\text{-C}(4) = 2.031(4)$, $\text{Fe}(1)\text{-C}(5) = 2.038(4)$, $\text{Fe}(1)\text{-C}(6) = 2.133(4)$ Å] are slightly shorter than those of the corresponding Fe-C bond distances in **1a**. One interesting finding is that among the phenazine carbon atoms coordinated to Fe(1) atom, the two C-C bond lengths are approximately equal [$\text{C}(3)\text{-C}(4) = 1.409(5)$, $\text{C}(5)\text{-C}(6) = 1.416(5)$ Å] and slightly longer than that of the other carbon-carbon bond distance [$\text{C}(4)\text{-C}(5) = 1.392(5)$ Å] define by the diene linkage in **4a**. The Fe-P bond distance is 2.2081(12). The remaining bond distances and angles are unremarkable and require no comment.

The spectroscopic data of **4a** are fully consistent with the solid-state structure. The IR spectra of compounds **4a** and **5a** exhibit a similar pattern of CO stretches, indicating that the number and arrangement of CO ligands are similar in both the species. In addition to the characteristic phenyl and phenazine ring proton resonances in the aromatic region, the aliphatic region of ^1H NMR of **4a** displays diastereotopic protons at δ 3.23 and 3.04 (each integrating to 1H) assigned to the methylene protons of the dppm ligand. In each of **4a** and **5a**, the presence of a dangling diphosphine is easily deduced from the $^{31}\text{P}\{^1\text{H}\}$ NMR spectra,

which exhibit two doublets at δ 57.0 and -24.0 ($J = 76.0$ Hz) for **4a** and two singlets δ 61.0 and -18.1 for **5a**, consistent with the presence of two nonequivalent phosphorus nuclei. The higher field resonance in each species is confidently assigned to the dangling phosphine moiety.

4. Conclusions

A summary of the reactions described in this report is shown in Schemes 3 and 4. The reaction of phenazine and acridine with $\text{Fe}_3(\text{CO})_{12}$ at 80 °C yielded the mononuclear complexes $\text{Fe}(\text{CO})_3(\eta^4\text{-C}_{12}\text{H}_8\text{N}_2)$ (**1a**) and $\text{Fe}(\text{CO})_3(\eta^4\text{-C}_{13}\text{H}_9\text{N})$ (**1b**) as the sole isolable products. Four new substituted derivatives $\text{Fe}(\text{CO})_2\text{P}(\eta^4\text{-heterocycle})$ [where P = $\text{P}(\text{OMe})_3$ and PPh_3] were prepared from **1a** and **1b** by oxidative decarbonylation of the parent compound upon treatment of Me_3NO in the presence of a P-donor. Similar reactions between **1a** and **1b** and the diphosphines dppm and dppf were also confirmed. The η^4 -coordination of a phenazine and acridine ligand to the iron center in our new compounds is unprecedented, and we have structurally established this phenomenon in for compounds **1a**, **2a**, **3b**, and **4a**. The stability of the ancillary phenazine and acridine ligands in arene exchange reactions and site-selective functionalization of the coordinated heterocycle are presently under investigation.

5. Acknowledgements

We thank the Ministry of Education, the Government of the People's Republic of Bangladesh for financial support. MGR thanks the Robert A. Welch Foundation (grant B-1093) for financial support and acknowledges computational resources through UNT's High Performance Computing Services and CASCaM. Prof. Michael B. Hall (TAMU) is thanked for providing us a copy of his *JIMP2* program, which was used to prepare the geometry-optimized structure reported here.

6. Appendix A. Supplementary material

CCDC,CCDC,CCDC and CCDC.....contain supplementary crystallographic data for **1a**, **2a**, **3b** and **4a** successively. These data may be obtained free of charge from The Cambridge Crystallographic Data Center via www.ccdc.cam.ac.uk/data_request/cif.

Table 1. Crystal data, data collection and structure refinement parameters for compounds **1a**, **2a**, **3b** and **4a**.

Compound	1a	2a	3b	4a
CCDC registry num.	str0828	xstr0029	xstr0324	str0971
Empirical formula	C ₁₅ H ₈ FeN ₂ O ₃	C ₁₇ H ₁₇ FeN ₂ O ₅ P	C ₃₃ H ₂₄ FeNO ₂ P	C ₄₂ H ₃₄ Cl ₂ FeO ₂ P ₂
Formula weight	320.08	416.15	553.35	759.38
Temperature (K)	150(2) K	150(2) K	150(1) K	150(2) K
Wavelength (Å)	Mo Kα, 0.71073	Cu Kα, 1.54184	Cu Kα, 1.54184	MoKα, 0.71073
Crystal system	triclinic	monoclinic	monoclinic	monoclinic
Space group	<i>P</i> 1 bar	<i>P</i> 2 ₁	<i>P</i> 2 ₁ / <i>n</i>	<i>C</i> 2/ <i>c</i>
a (Å)	6.7417(14) Å	6.99641(12)	16.29543(16)	32.239(11) Å
b (Å)	9.7046(19) Å	12.87326(19)	8.77976(7)	10.557(4) Å
c (Å)	10.249(2) Å	9.95847(17)	18.33151(16)	21.580(7) Å
α (°)	75.491(3) ^o	90	90	90 ^o
β (°)	86.227(3) ^o	99.3910(16)	99.0887(9)	108.522(5) ^o
γ (°)	86.227(3) ^o	90	90	90 ^o
Volume (Å ³)	644.4(2)	884.90(3)	2589.76(4)	6964(4)
Z	2	2	4	8
Calculated density (g/cm ³)	1.650	1.5617	1.419	1.448
Absorption coefficient (mm ⁻¹)	1.181	7.974	5.505	0.716
F(000)	324	427.6	1144.0	3136
Crystal size mm ³	0.14 × 0.10 × 0.09	0.3492 × 0.3013 × 0.1082	0.2 × 0.18 × 0.04	0.65 × 0.40 × 0.18
θ range for data collection (°)	3.56 to 28.20	12.82 to 147.92	6.748 to 147.248	2.01 to 28.58
Limiting indices	-8 ≤ h ≤ 8 -12 ≤ k ≤ 12 -13 ≤ l ≤ 13	-8 ≤ h ≤ 8 -11 ≤ k ≤ 16 -12 ≤ l ≤ 11	-20 ≤ h ≤ 19 -10 ≤ k ≤ 10 -22 ≤ l ≤ 22	-42 ≤ h ≤ 42 -13 ≤ k ≤ 13 -28 ≤ l ≤ 28
Reflections collected	5325	5128	45422	28345
Independent reflections (<i>R</i> _{int})	2822 [0.0201]	2597 [0.0342]	5182 [0.0360]	8265 [0.0648]
Completeness to theta	=26.00°, 96.1 %			= 26.00, 99.4 %
Refinement method	Full-matrix least-squares on <i>F</i> ²	Full-matrix least-squares on <i>F</i> ²		Full-matrix least-squares on <i>F</i> ²
Data / restraints / parameters	2822 / 0 / 222	2597 / 0 / 237	5182/0/343	8265 / 0 / 442
Goodness-of-fit on <i>F</i> ²	2544	1.053	1.133	4988
Final R indices [<i>I</i> > 2σ(<i>I</i>)]	<i>R</i> ₁ = 0.0350, <i>wR</i> ₂ = 0.0933	<i>R</i> ₁ = 0.0369, <i>wR</i> ₂ = 0.0945	<i>R</i> ₁ = 0.0348 <i>wR</i> ₂ = 0.0816	<i>R</i> ₁ = 0.0637, <i>wR</i> ₂ = 0.1595
R indices (all data)	<i>R</i> ₁ = 0.0388, <i>wR</i> ₂ = 0.0965	<i>R</i> ₁ = 0.0378, <i>wR</i> ₂ = 0.0957	<i>R</i> ₁ = 0.0364 <i>wR</i> ₂ = 0.0824	<i>R</i> ₁ = 0.1070, <i>wR</i> ₂ = 0.1795
Largest diff. peak/hole (e.Å ⁻³)	0.705 and -0.462	1.21 and -0.62	0.41/-0.33	1.285 and -0.699

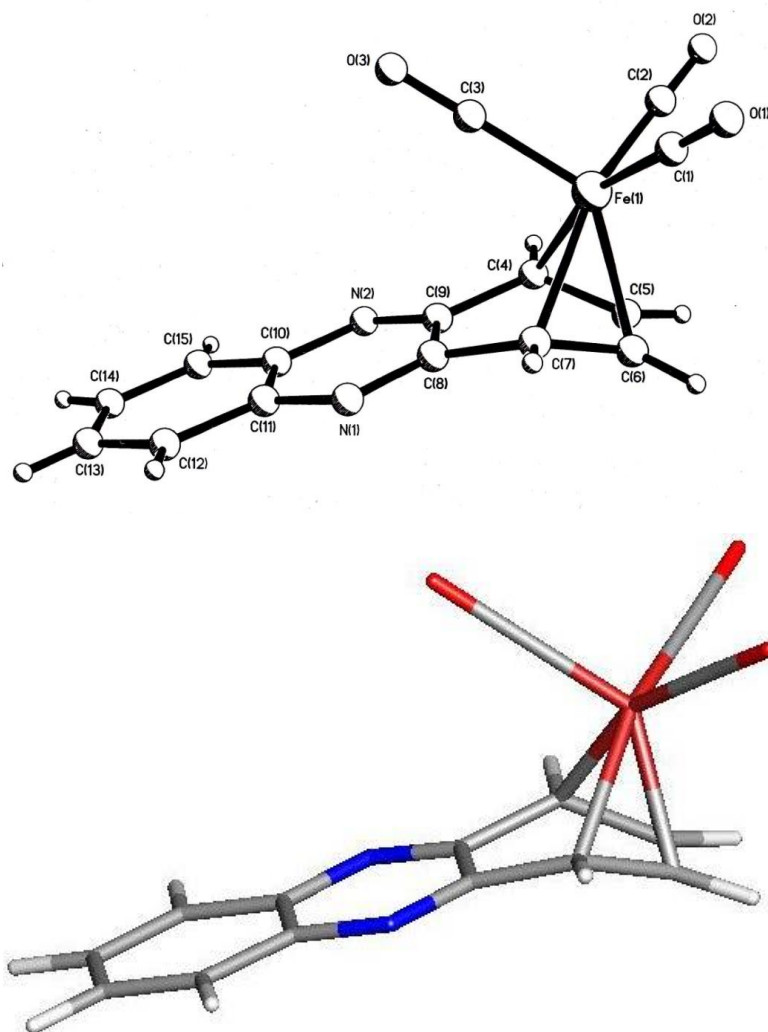


Fig. 1. ORTEP drawing of the molecular structure of $\text{Fe}(\text{CO})_3(\eta^4\text{-C}_{12}\text{H}_8\text{N}_2)$ (**1a**; top) and DFT-optimized structure of **A** (bottom). Selected X-ray diffraction bond lengths (\AA) and angles ($^\circ$): Fe(1)-C(5) 2.0549(19), Fe(1)-C(6) 2.057(2), Fe(1)-C(4) 2.154(2), Fe(1)-C(7) 2.156(2), N(1)-C(8) 1.308(2), N(1)-C(11) 1.386(2), N(2)-C(9) 1.312(2), N(2)-C(10) 1.394(2), C(4)-C(5) 1.430(3), C(4)-C(9) 1.468(2), C(5)-C(6) 1.395(3), C(6)-C(7) 1.425(3), C(7)-C(8) 1.471(3), C(8)-C(9) 1.432(3), C(10)-C(11) 1.403(3), C(12)-C(13) 1.377(3), C(13)-C(14) 1.393(3), C(14)-C(15) 1.376(3), C(2)-Fe(1)-C(1) 91.51(10), C(2)-Fe(1)-C(3) 100.58(9), C(1)-Fe(1)-C(3) 99.56(9), C(2)-Fe(1)-C(5) 93.34(9), C(1)-Fe(1)-C(5) 124(9), C(3)-Fe(1)-C(5) 133.57(9), C(2)-Fe(1)-C(6) 122.76(9), C(1)-Fe(1)-C(6) 94.26(9), C(3)-Fe(1)-C(6) 134.03(9), C(5)-Fe(1)-C(6) 39.68(8), C(2)-Fe(1)-C(4) 93.95(8), C(1)-Fe(1)-C(4) 163.29(9), C(3)-Fe(1)-C(4) 94.94(9), C(5)-Fe(1)-C(4) 39.64(8), C(6)-Fe(1)-C(4) 69.55(8), C(2)-Fe(1)-C(7) 161.87(9), C(1)-Fe(1)-C(7) 93.49(9), C(3)-Fe(1)-C(7) 95.76(8), C(5)-Fe(1)-C(7) 69.52(8), C(6)-Fe(1)-C(7) 39.47(8), C(4)-Fe(1)-C(7) 76.75(8).

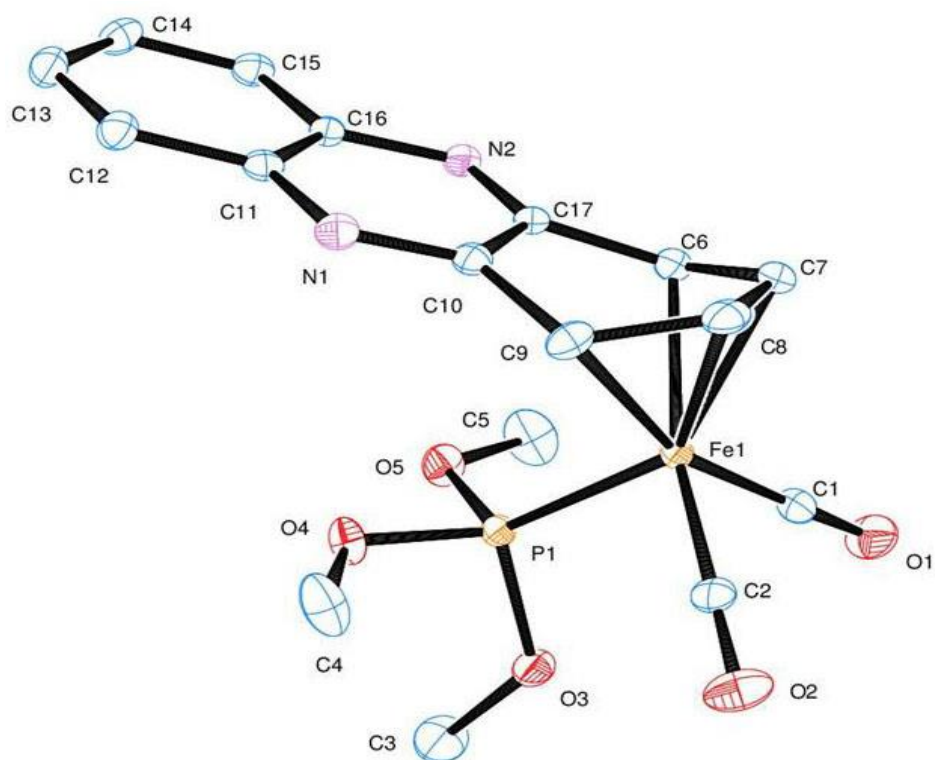


Fig. 2. ORTEP drawing of the molecular structure of $\text{Fe}(\text{CO})_2\{\text{P}(\text{OMe})_3\}(\eta^4\text{-C}_{12}\text{H}_8\text{N}_2)$ (**2a**). Hydrogen atoms are omitted for clarity. Selected bond lengths (\AA) and angles ($^\circ$): $\text{Fe}(1)\text{-P}(1)$ 2.1647(6), $\text{Fe}(1)\text{-C}(1)$ 1.773(4), $\text{Fe}(1)\text{-C}(2)$ 1.772(4), $\text{Fe}(1)\text{-C}(6)$ 2.153(4), $\text{Fe}(1)\text{-C}(7)$ 2.048(4), $\text{Fe}(1)\text{-C}(8)$ 2.050(4), $\text{Fe}(1)\text{-C}(9)$ 2.153(4), $\text{C}(14)\text{-C}(15)$ 1.376(5), $\text{C}(15)\text{-C}(16)$ 1.396(5), $\text{N}(1)\text{-C}(10)$ 1.308(5), $\text{N}(1)\text{-C}(11)$ 1.371(4), $\text{N}(2)\text{-C}(16)$ 1.394(4), $\text{N}(2)\text{-C}(17)$ 1.305(5), $\text{C}(6)\text{-C}(7)$ 1.428(5), $\text{C}(6)\text{-C}(17)$ 1.472(5), $\text{C}(7)\text{-C}(8)$ 1.408(4), $\text{C}(8)\text{-C}(9)$ 1.423(5), $\text{C}(9)\text{-C}(10)$ 1.453(5), $\text{C}(10)\text{-C}(17)$ 1.454(3), $\text{C}(11)\text{-C}(12)$ 1.411(5), $\text{C}(11)\text{-C}(16)$ 1.420(3), $\text{C}(12)\text{-C}(13)$ 1.369(5), $\text{C}(13)\text{-C}(14)$ 1.405(4), $\text{C}(1)\text{-Fe}(1)\text{-P}(1)$ 95.94(13), $\text{C}(2)\text{-Fe}(1)\text{-P}(1)$ 96.18(13), $\text{C}(2)\text{-Fe}(1)\text{-C}(1)$ 90.99(11), $\text{C}(8)\text{-Fe}(1)\text{-P}(1)$ 138.75(11), $\text{C}(9)\text{-Fe}(1)\text{-P}(1)$ 99.77(11).

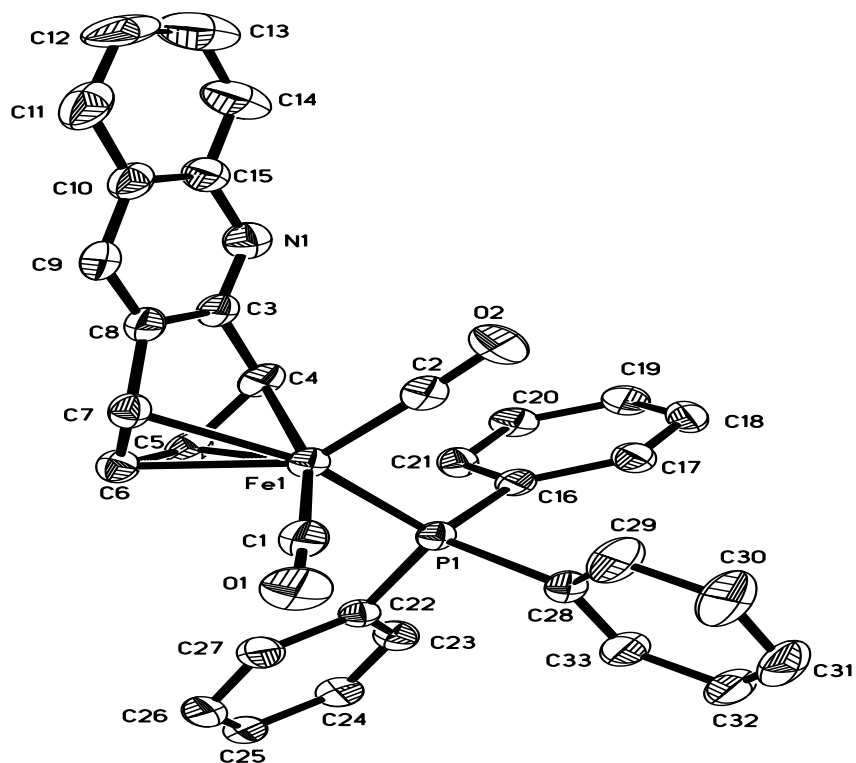


Fig. 3. ORTEP drawing of the molecular structure of $\text{Fe}(\text{CO})_2(\text{PPh}_3)(\eta^4\text{-C}_{13}\text{H}_9\text{N})$ (**3b**), Hydrogen atoms are omitted for clarity. Selected bond lengths (\AA) and angles ($^\circ$): Fe(1)-P(1) 2.2277(6), Fe(1)-C(4) 2.1585(19), Fe(1)-C(5) 2.054(2), Fe(1)-C(6) 2.051(2), Fe(1)-C(7) 2.143(2), N(1)-C(3) 1.321(3), N(1)-C(15) 1.399(3), C(3)-C(4) 1.469(3), C(4)-C(5) 1.422(3), C(5)-C(6) 1.406(3), C(6)-C(7) 1.432(3), C(7)-C(8) 1.466(3), C(3)-C(8) 1.434(3), C(4)-Fe(1)-P(1) 97.90(6), C(5)-Fe(1)-P(1) 92.74(6), C(5)-Fe(1)-C(4) 39.35(8), C(5)-Fe(1)-C(7) 69.78(8), C(6)-Fe(1)-P(1) 119.05(7), C(6)-Fe(1)-C(4) 69.60(8), C(6)-Fe(1)-C(5) 40.07(9), C(6)-Fe(1)-C(7) 39.86(9), C(7)-Fe(1)-P(1) 158.90(6), C(7)-Fe(1)-C(4) 76.33(8), C(6)-C(7)-Fe(1) 66.59(11), C(6)-C(7)-C(8) 119.87(18), C(8)-C(7)-Fe(1) 104.24(13), C(3)-C(8)-C(7) 114.45(18), C(9)-C(8)-C(3) 120.0(2), C(9)-C(8)-C(7) 125.44(19), C(8)-C(9)-C(10) 118.6(2), N(1)-C(3)-C(4) 121.45(18), N(1)-C(3)-C(8) 123.56(19), C(8)-C(3)-C(4) 114.88(18), C(3)-C(4)-Fe(1) 103.35(12), C(5)-C(4)-Fe(1) 66.35(11), C(5)-C(4)-C(3) 119.80(19), C(4)-C(5)-Fe(1) 74.31(11), C(6)-C(5)-Fe(1) 69.85(12), C(6)-C(5)-C(4) 116.45(19), C(5)-C(6)-Fe(1) 70.08(12), C(5)-C(6)-C(7) 115.60(19), C(7)-C(6)-Fe(1) 73.56(12).

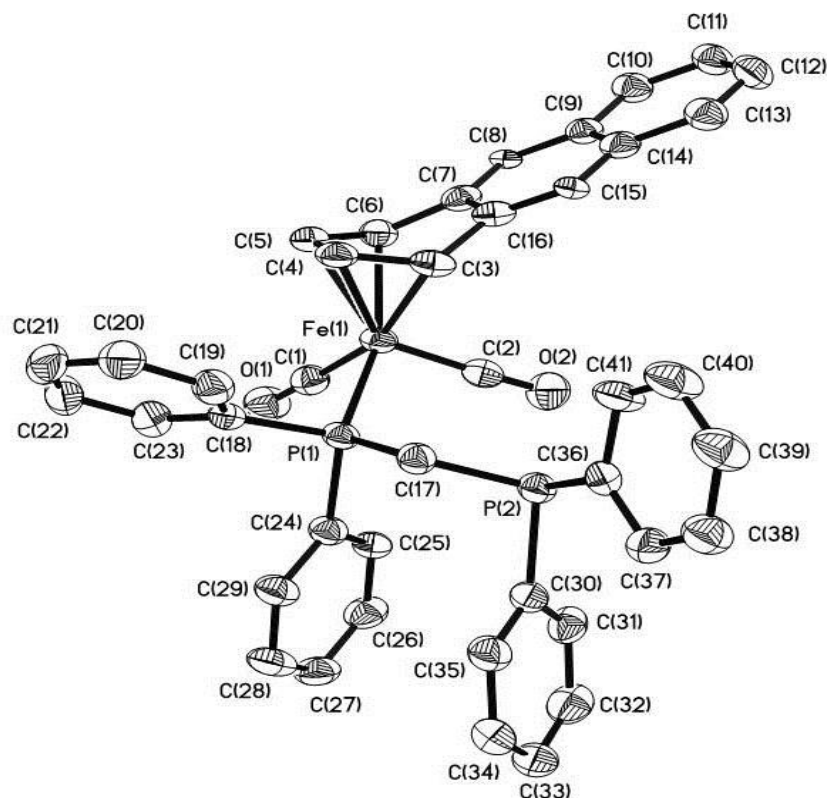


Fig. 4. ORTEP drawing of the molecular structure of $\text{Fe}(\text{CO})_2(\text{dppm})(\eta^4\text{-C}_{12}\text{H}_8\text{N}_2)$ (**4a**). Hydrogen atoms are omitted for clarity. Selected bond lengths (\AA) and angles ($^\circ$): $\text{Fe}(1)\text{-C}(1)$ 1.758(4), $\text{Fe}(1)\text{-C}(2)$ 1.773(4), $\text{Fe}(1)\text{-C}(4)$ 2.031(4), $\text{Fe}(1)\text{-C}(5)$ 2.038(4), $\text{Fe}(1)\text{-C}(3)$ 2.122(4), $\text{Fe}(1)\text{-C}(6)$ 2.133(4), $\text{Fe}(1)\text{-P}(1)$ 2.2081(12), $\text{C}(3)\text{-C}(4)$ 1.409(5), $\text{C}(3)\text{-C}(16)$ = 1.453(5), $\text{C}(4)\text{-C}(5)$ 1.392(5), $\text{C}(5)\text{-C}(6)$ 1.416(5), $\text{C}(6)\text{-C}(7)$ 1.451(5), $\text{C}(7)\text{-C}(8)$ 1.283(5), $\text{C}(7)\text{-C}(16)$ 1.452(5), $\text{C}(8)\text{-C}(9)$ 1.366(5), $\text{C}(9)\text{-C}(10)$ 1.405(5), $\text{C}(9)\text{-C}(14)$ 1.408(5), $\text{C}(10)\text{-C}(11)$ = 1.359(5), $\text{C}(11)\text{-C}(12)$ 1.398(6), $\text{C}(12)\text{-C}(13)$ 1.375(6), $\text{C}(1)\text{-Fe}(1)\text{-C}(2)$ 100.73(17), $\text{C}(1)\text{-Fe}(1)\text{-C}(4)$ 123.03(17), $\text{C}(2)\text{-Fe}(1)\text{-C}(4)$ 134.58(16), $\text{C}(1)\text{-Fe}(1)\text{-C}(5)$ 92.71(16), $\text{C}(2)\text{-Fe}(1)\text{-C}(5)$ 137.41(16), $\text{C}(4)\text{-Fe}(1)\text{-C}(5)$ 40.01(15), $\text{C}(1)\text{-Fe}(1)\text{-C}(3)$ 162.11(16), $\text{C}(2)\text{-Fe}(1)\text{-C}(3)$ 95.54(16), $\text{C}(4)\text{-Fe}(1)\text{-C}(3)$ 39.60(15), $\text{C}(5)\text{-Fe}(1)\text{-C}(3)$ 70.09(15), $\text{C}(1)\text{-Fe}(1)\text{-C}(6)$ 93.04(16), $\text{C}(2)\text{-Fe}(1)\text{-C}(6)$ 98.96(16), $\text{C}(4)\text{-Fe}(1)\text{-C}(6)$ 69.59(15), $\text{C}(5)\text{-Fe}(1)\text{-C}(6)$ 39.62(15), $\text{C}(3)\text{-Fe}(1)\text{-C}(6)$ 76.99(15), $\text{C}(1)\text{-Fe}(1)\text{-P}(1)$ 89.19(13), $\text{C}(2)\text{-Fe}(1)\text{-P}(1)$ 100.29(12), $\text{C}(4)\text{-Fe}(1)\text{-P}(1)$ 92.47(12), $\text{C}(5)\text{-Fe}(1)\text{-P}(1)$ 120.30(12), $\text{C}(3)\text{-Fe}(1)\text{-P}(1)$ 95.22(11), $\text{C}(6)\text{-Fe}(1)\text{-P}(1)$ 159.85(11).

References

-
- ¹ R.M. Hochstrasser, *J. Chem. Phys.* 36 (1962) 1808.
- ² A.J. Kallir, G.W. Suter, U.P. Wild, *J. Phys. Chem.* 89 (1985) 1996.
- ³ J.J. Aaron, M. Maafi, C.Parkanyi, C. Boniface, *Spectrochim. Acta* 51A (1995) 603.
- ⁴ Y. Hirata, I. Tanaka, *Chem. Phys. Lett.* 43 (1976) 568.
- ⁵ A. Grabowska, *Chem. Phys. Lett.* 1 (1967) 1113.
- ⁶ T.G. Pavlopoulos, *Spectrochim. Acta* 43A (1987) 715.
- ⁷ J.I. Del Barrio, J.R. Rebato, F.M.G.- Tablas, *J. Phys. Chem.*, 1989, **93**, 6836.
- ⁸ V.A. Kuzmin, P.P. Levin, *Bull. Acad. Sci. USSR Div. Chem. Sci.* 1988, **37**, 1098.
- ⁹ (a) W. Maniukiewicz, M. Bukowska-Strzyzewska, M. Sadowska, *Acta Cryst. E* 60 (2004) m73. (b) R.T. Schneider, C.P. Landee, M.M. Turnbull, F.F. Awwadi, B. Twamley, *Polyhedron* 26 (2007) 1849.
- ¹⁰ (a) F.A. Cotton, T.R. Felthouse, *Inorg. Chem.* 20 (1981) 600. (b) F.A. Cotton, Y. Kim, T. Ren, *Inorg. Chem.* 31 (1992) 2723. (c) J. Scholz, A. Scholz, R. Weimann, C. Janiak, H. Schumann, *Angew. Chem., Int. Ed.* 33 (1994) 1171. (d) M. Munakata, T. Kuroda-Sowa, M. Maekawa, A. Honda, S. Kitagawa, *J. Chem. Soc., Dalton Trans.* (1994) 2771. (e) T. Kuroda-Sowa, M. Munakata, H. Matsuda, S. Akiyama, M.J. Maekawa, *J. Chem. Soc., Dalton Trans.* (1995) 2201. (f) J.A. Whiteford, P.J. Stang, S.D. Huang, *Inorg. Chem.* 37 (1998) 5595. (g) S.R. Batten, B.F. Hoskins, R. Robson, *New J. Chem.* 22 (1998) 173. (h) D.J. Chesnut, D. Plewak, J. Zubieta, *J. Chem. Soc., Dalton Trans.* (2001) 2567. (i) H. Miyasaka, R. Clerac, C.S. Campos-Fernández, K.R. Dunbar, *J. Chem. Soc., Dalton Trans.* (2001) 858. (j) Z. Shi, X. Gu, J. Peng, Z. Xin, *Eur. J. Inorg. Chem.* (2005) 3811. (k) T. Kogane, N. Koyama, T. Ishida, T. Nogami, *Polyhedron* 26 (2007), 1811. (l) J.Q. Sha, J. Peng, A.X. Tian, H.S. Liu, J. Chen, *Cryst. Growth Des.* 7 (2007). 2535. (m) T. Schneider, C.P. Landee, M.M. Turnbull, F.F. Awwadi, B. Twamley, *Polyhedron* 26 (2007) 1849. (n) J. Q. Sha, J. Peng, Y. Li, P. P. Zhang, H. J. Pang, *Inorg. Chem. Commun.* 11 (2008) 907. (o) S.E.H. Etaiw, D.M.A. El-Aziz, M.S. Ibrahim, A.S.B. El-din, *Polyhedron* 28 (2009) 1001. (p) W.J. Evans, S.E. Lorenz, J.W. Ziller, *Inorg. Chem.* 48 (2009) 2001.

-
- ¹¹ M. Munakata, S. Kitagawa, N. Ujimarui, M. Nakamura, M. Maekawa, H. Matsuda, *Inorg. Chem.* 32 (1993) 826.
- ¹² F.A. Cotton, G. Wilkinson, *Advanced Inorganic Chemistry*, 5th ed.; John Wiley & Sons: New York, 1988. (b) N.N. Greenwood, A. Earnshaw, *Chemistry of the Elements*, Pergamon Press: Oxford, U.K., 1984.
- ¹³ U. R. Chaudhuri, *Fundamentals of Petroleum and Petrochemical Engineering*, CRC Press: Boca Raton, FL, 2011.
- ¹⁴ M.I. Bruce, M.G. Humphrey, M. R. Snow, E.R.T. Tiekink, R.C. Wallis, *J. Organomet. Chem.* 314 (1986) 311.
- ¹⁵ N.E. Leadbeater, J. Lewis, P.R. Raithby, G.N. Ward, *J. Chem. Soc., Dalton Trans.* (1997) 2511.
- ¹⁶ D. Ellis, L.F. Farrugia, *J. Cluster. Sci.*, 7 (1996) 71.
- ¹⁷ A. Eisenstadt, C.M. Giandomenico, M.F. Frederick, R.M. Laine, *Organometallics*, 1985, **4**, 2033.
- ¹⁸ G.A. Foulds, B.F.G. Johnson, J. Lewis, *J. Organomet. Chem.* 294 (1985) 123.
- ¹⁹ J.A. Cabeza, I. del Río, E. Pérez-Carreño, V. Pruneda, *Organometallics*, 30 (2011) 1148.
- ²⁰ J.A. Cabeza, I. del Río, M.C. Goite, E. Pérez-Carreño, V. Pruneda, *Chem. Eur. J.* 15 (2009) 7339.
- ²¹ A. Eisenstadt, C.M. Giandomenico, M.F. Frederick, R.M. Laine, *Organometallics* 4 (1985) 2033.
- ²² C.C. Yin, A.J. Deeming, *J. Chem. Soc., Dalton Trans.* (1975) 2091.
- ²³ R.H. Fish, T.J. Kim, J.L. Steward, J.H. Bushweller, R.K. Rosen, J. W. Dupon. *Organometallics*, 5 (1986) 2193.
- ²⁴ J.A. Cabeza, P. Garcia-Alvarez, V. Pruneda, *Organometallics*, 31 (2012) 941.
- ²⁵ Md. A. H. Chowdhury, S. Rajbangshi, A. Rahaman, L. Yang, V. N. Nesterov, M. G. Richmond, S. M. Mobin, S. E. Kabir, *J. Organomet. Chem.* 779 (2015) 21.
- ²⁶ W. McFarlane, G. Wilkinson, *Inorg. Synth.* 8 (1966) 181.

-
- ²⁷ M. J. Frisch, G. W. Trucks, H. B. Schlegel, G. E. Scuseria, M. A. Robb, J. R. Cheeseman, G. Scalmani, V. Barone, B. Mennucci, G. A. Petersson, H. Nakatsuji, M. Caricato, X. Li, H. P. Hratchian, A. F. Izmaylov, J. Bloino, G. Zheng, J. L. Sonnenberg, M. Hada, M. Ehara, K. Toyota, R. Fukuda, J. Hasegawa, M. Ishida, T. Nakajima, Y. Honda, O. Kitao, H. Nakai, T. Vreven, J. A. Montgomery, Jr., J. E. Peralta, F. Ogliaro, M. Bearpark, J. J. Heyd, E. Brothers, K. N. Kudin, V. N. Staroverov, R. Kobayashi, J. Normand, K. Raghavachari, A. Rendell, J. C. Burant, S. S. Iyengar, J. Tomasi, M. Cossi, N. Rega, J. M. Millam, M. Klene, J. E. Knox, J. B. Cross, V. Bakken, C. Adamo, J. Jaramillo, R. Gomperts, R. E. Stratmann, O. Yazyev, A. J. Austin, R. Cammi, C. Pomelli, J. W. Ochterski, R. L. Martin, K. Morokuma, V. G. Zakrzewski, G. A. Voth, P. Salvador, J. J. Dannenberg, S. Dapprich, A. D. Daniels, O. Farkas, J. B. Foresman, J. V. Ortiz, J. Cioslowski, D. J. Fox, Gaussian 09, Revision A.02, Gaussian, Inc., Wallingford CT, 2009.
- ²⁸ A. D. Becke, *J. Chem. Phys.* 98 (1993) 5648.
- ²⁹ C. Lee, W. Yang, R. G. Parr, *Phys. Rev. B* 37 (1988), 785.
- ³⁰ (a) M. Dolg, U. Wedig, H. Stoll, H. Preuss, *J. Chem. Phys.* 86 (1987) 866. (b) S. P. Walch, C. W. Bauschlicher, *J. Chem. Phys.* 78 (1983) 4597.
- ³¹ (a) G. A. Petersson, A. Bennett, T. G. Tensfeldt, M. A. Al-Laham, W. A. Shirley, J. Mantzaris, *J. Chem. Phys.* 89 (1988) 2193. (b) G. A. Petersson, M. A. Al-Laham, *J. Chem. Phys.* 94 (1991) 6081.
- ³² A.E. Reed, L.A. Curtiss, F. Weinhold, *Chem. Rev.* 88 (1988) 899.
- ³³ K.B. Wiberg, *Tetrahedron* 24 (1968) 1083.
- ³⁴ (a) JIMP2, version 0.091, a free program for the visualization and manipulation of molecules: M. B. Hall, R. F. Fenske, *Inorg. Chem.* 11 (1972) 768. (b) J. Manson, C. E. Webster, M. B. Hall, Texas A&M University, College Station, TX, 2006:
<http://www.chem.tamu.edu/jimp2/index.html>.
- ³⁵ A. Sattler, G. Zhu, G. Parkin, *J. Am. Chem. Soc.* 131 (2009) 7828.
- ³⁶ Q. Dong, J.-H. Su, S. Gong, Q.-S. Li, Y. Zhao, B. Wu, X.-J. Yang, *Organometallics* 32 (2013) 2866.

-
- ³⁷ (a) G.J. Reiss, *Acta Crystallogr. Sect. E Struct. Rep. Online* 66 (2010) m1369 and references therein. (b) S.L. Ingham, S.W. Magennis, *J. Organomet. Chem.* 574 (1999) 302. (c) K.S. Claire, O.W. Howarth, A. McCamley, *J. Chem. Soc., Dalton Trans.* (1994) 2615. (d) R. Goddard, P. Woodward, *J. Chem. Soc., Dalton Trans.* (1979) 661. (e) T. Ando, N. Nakata, K. Suzuki, T. Matsumoto, *J. Chem. Soc., Dalton Trans.* 41 (2012) 1678.
- ³⁸ (a) T.A. Albright, P. Hofmann, R. Hoffmann, *J. Am. Chem. Soc.* 99 (1977) 7546. (b) M. Bühl, W. Thiel, *Inorg. Chem.* 36 (1997) 2922.
- ³⁹ L. Kruczynski, J. Takats, *Inorg. Chem.* 15 (1976) 3140.
- ⁴⁰ H.Ye. Liu, Md.M. Rahman, L.L. Koh, K. Eriks, W.P. Giering, A. Prock, *Acta. Cryst. C* 45 (1989) 1683.
- ⁴¹ D.L. Reger, E. Mintz, L. Lebioda, *J. Am. Chem. Soc.* 108 (1986) 1940.